



Biodiesel production from the microalgae *Nannochloropsis gaditana*: Optimization of the transesterification reaction and physicochemical characterization

C. Sanjurjo^a, P. Oulego^b, M. Bartolomé^c, E. Rodríguez^{a,*}, R. Gonzalez^c, A. Hernández Battez^a

^a Department of Construction and Manufacturing Engineering, University of Oviedo, Pedro Puig Adam, s/n, 33203, Gijón, Spain

^b Department of Chemical and Environmental Engineering, University of Oviedo, C/Julián Clavería s/n, E-33071, Oviedo, Spain

^c Department of Marine Science and Technology, University of Oviedo, Blasco de Garay, s/n, 33203, Gijón, Spain

ARTICLE INFO

Keywords:

Biodiesel
Microalgae
Transesterification
Optimization
Response surface methodology

ABSTRACT

The current environmental scenario has encouraged the study of renewable and competitive alternative feedstocks for biodiesel production. Microalgae present a significant opportunity as a feedstock that does not require arable land and can be cultivated using wastewater. The paper investigates the optimization of biodiesel production from microalgae *Nannochloropsis gaditana* bio-oil using response surface methodology and also analyzes the main physicochemical properties of the bio-oil. It was confirmed that this methodology is suitable for materials with low homogeneity. The model is also adequate for determining optimal experimental conditions, resulting in a FAME content of 87.25 %. The biodiesel's physicochemical properties were analyzed. It was discovered that the high degree of unsaturation in the microalgae bio-oil's chemical structure resulted in a narrower temperature range for its application compared to other vegetable sources.

1. Introduction

The energy industry has shown clear evidence of the urgent need for change over the past decade due to fuel price inflation and the environmental impact of global warming. As fossil resources become scarcer, attention has turned to more environmentally friendly alternatives, such as natural-based biodiesel. Biodiesel, defined by ASTM D6751 [1], refers to mono-alkyl esters of fatty acids derived from vegetable oils and animal fats. Biofuels offer several advantages over petroleum-based fuels. They are more efficient, have lower sulfur and aromatic content, better lubricity, higher cetane number, higher flash point, and a positive energy balance [2,3]. Furthermore, biofuels are renewable, portable, non-toxic, non-flammable, biodegradable, and reduce most regulated exhaust emissions. Additionally, using vegetable-based sources can help grow rural economies and reduce reliance on petroleum-based fuels, ultimately lowering the cost of the final product [4]. However, biodiesel has limitations due to poor flow properties at low temperatures, inadequate storage performance caused by low oxidative stability, and potential NOx emissions, especially when used in older engines without new emission reduction technologies [2].

The four main categories of biodiesel are based on the feedstock

used: 1st generation, which uses edible crops; 2nd generation, which uses non-edible crops that require arable land; 3rd generation, which is derived from microalgae, bacteria, fungi, etc.; and 4th generation, which uses genetically modified microalgae [5]. The 1st generation satisfies over two-thirds of the world's bioenergy needs and comprises all arable crops [4,6]. The use of plant resources for energy production has raised concerns about competition with food sources and water supplies. This highlights the problem of water and food scarcity in today's world [7,8]. Increased production costs and higher food prices have resulted. The 2nd generation of plant-based energy sources was developed to address the limitations of the 1st generation. This group includes animal fats, agricultural waste, and oil waste [3,9]. These products are easy to access and do not require investment in cultivation or harvesting since they are waste primary products. This reduces the overall process cost. However, their availability is not fixed and may be insufficient. Additionally, they require pre-treatment to remove any impurities present in the waste [7]. Third-generation biodiesel uses microalgae-derived biomass, which has the advantage of not requiring arable land. Microorganisms can grow in wastewater and absorb nutrients and impurities, making them useful for purifying polluted water [5,10]. The third generation of microorganisms is becoming more popular due to its advantages over the first and second

* Corresponding author.

E-mail address: eduardo@uniovi.es (E. Rodríguez).

<https://doi.org/10.1016/j.biombioe.2024.107240>

Received 3 January 2024; Received in revised form 24 April 2024; Accepted 2 May 2024

Available online 6 May 2024

0961-9534/© 2024 The Authors. Published by Elsevier Ltd. This is an open access article under the CC BY-NC-ND license (<http://creativecommons.org/licenses/by-nc-nd/4.0/>).

Table 1

Design of experiments for the optimization of biodiesel production from vegetable oils.

Feedstock	Experimental Design	Independent factors	Outputs	Ref.
<i>Chlorella protothecoides</i>	TR	Alcohol ratio (molar), temperature (°C), time (h)	Conversion rate (%)	[38]
<i>Nannochloropsis gaditana</i>	TR	Alcohol ratio (mL/g), temperature (°C), time (h)	Conversion rate (%)	[39]
Palm oil	TR	Catalyst calcination temperature (°C), catalyst (%), alcohol ratio (molar), temperature (°C), stirring speed (rpm)	FAME yield (%)	[40]
Rice bran	TR	Catalyst (g), alcohol ratio (ml)	Conversion rate (%)	[41]
<i>Chlorella vulgaris</i>	TR	Alcohol ratio (mL), temperature (°C), catalyst (%), time (min)	FAME yield (%)	[42]
<i>Chlorella vulgaris</i>	TR	Alcohol ratio (molar); temperature (°C), time (min)	FAME yield (%)	[43]
Waste cooking oil	TR	Alcohol ratio (molar), temperature (°C), time (min)	FAME content (%)	[44]
<i>Chlorella protothecoides</i>	TR	Alcohol ratio (molar), temperature (°C), catalyst (%)	Conversion rate (%)	[45]
<i>Jatropha curcas</i> <i>Elaeis guineensis</i> (palm)	RSM	Alcohol ratio (molar), catalyst (%)	FAME/FAEE content (%)	[46]
Sunflower oil	RSM	Alcohol ratio (molar), temperature (°C), catalyst (g)	Viscosity (cSt)	[47]
Refined soybean oil (RSO)	RSM	Alcohol ratio (molar), temperature (°C), catalyst (%), ultrasound power (W)	Conversion rate (%)	[48]
<i>Pistacia lentiscus</i>	RSM	Alcohol ratio (molar), temperature (°C), catalyst (%)	FAME yield (%)	[49]
Food grade refined palm oil (RPO)	RSM-CCD	Alcohol ratio (molar), temperature (°C) time (h), catalyst (%)	Conversion rate (%)	[36]
Neem oil	RSM-CCD	Alcohol ratio (molar), temperature (°C), time (h), catalyst (%), stirring speed (rpm)	Conversion rate (%)	[9]
Palm oil	RSM-CCD	Alcohol ratio (ml), time (min), catalyst (%)	FAME yield (%)	[50]
Rubber seed oil	RSM-CCD	Alcohol ratio (molar), temperature (°C), time (min), catalyst (%)	Conversion rate (%)	[51]

Table 1 (continued)

Feedstock	Experimental Design	Independent factors	Outputs	Ref.
<i>Chlorella vulgaris</i> + castor oil	RSM-CCD	Alcohol ratio (mL), temperature (°C), catalyst (%)	Conversion rate (%)	[52]
<i>Chlorella protothecoides</i>	RSM-CCD	Alcohol ratio (mol/mol), temperature (°C), residence time (min), pressure (bar), water content (wt%)	FAME yield (%)	[53]
<i>Chlorella variabilis</i>	RSM-CCD	Alcohol ratio (molar), temperature (°C), time (min), catalyst (wt%)	FAME yield (%)	[54]
<i>Spirulina platensis</i>	RSM-CCD	Alcohol ratio (mL/g), temperature (°C), co-solvent ratio (mL/g), time (min), water content (%)	FAME yield (%)	[55]
<i>Brassica campestris</i>	RSM-CCRD	Alcohol ratio (molar), temperature (°C), time (min), catalyst (%)	Conversion rate (%) Viscosity (mm ² /s) Cetane number	[56]
<i>Spirogyra crassa</i>	RSM-CCRD	Alcohol ratio (molar), temperature (°C), time (min), catalyst (%)	FAME yield (%)	[57]
Palm oil	RSM-BBD	EFI (V/cm), time (min)	Conversion rate (%)	[58]
Palm oil	RSM-BBD	Alcohol ratio (molar), temperature (°C), time (min)	FAME yield (%)	[34]
<i>Nannochloropsis gaditana</i>	RSM-BBD	Alcohol ratio (mL/g), catalyst (%), hexane/SL ratio (mL/g)	FAME yield (%)	[59]

homogeneous materials, such as microalgae oils. In most cases, researchers preferred the central composite design (CCD) as the experimental design when dealing with fewer than four independent variables. CCD was used by Nan et al. [53], Nirmala et al. [54], and Mohamadzadeh et al. [55] to optimize the transesterification reaction and achieve the highest FAME yield in microalgae, such as *C. protothecoides*, *C. variabilis*, and *S. platensis*. Beyene et al. [52] used RSM via CCD to optimize the production of biodiesel from a mixture of castor oil and the microalgae *C. vulgaris*.

Macías-Sánchez et al. [59,60] conducted two studies to optimize the FAME yield of direct transesterification of wet *N. gaditana* biomass. In the first study, they optimized temperature and reaction time using a simple experimental design without RSM [60]. Later, they applied RSM-CCD to optimize the catalyst concentration, alcohol, and hexane ratio on the same material, using the optimal conditions of temperature and reaction time obtained in the first study [59].

The aim of this work is to optimize the production of biodiesel from the bio-oil extracted from the microalgae *Nannochloropsis gaditana* (*N. gaditana*) through transesterification. The study focused solely on microalgae bio-oil, not wet biomass. All independent variables, including alcohol ratio, temperature, and reaction time, were optimized in a single study. A physicochemical characterization was performed to fully understand the resulting product.

Table 2
Input variables and levels for optimizing the MBO transesterification reaction.

Input variables	Factor	Variable levels				
		-2 (-α)	-1	0	+1	+2 (+α)
Bio-oil:methanol ratio	A	1:3	1:6	1:9	1:12	1:15
Reaction temperature (°C)	B	30	50	70	90	110
Reaction time (min)	C	30	67.5	105	142.5	180

Table 3
Design of experiments and responses.

Std. order	Run order	Factorial input variable			Responses, Y		
		A	B	C	Actual	Predicted	
					Y (%)	Y (%)	Error (%)
11	1	0	-2	0	81.81	84.18	2.90
18	2	0	0	0	78.52	78.90	0.49
2	3	1	-1	-1	86.99	88.87	2.16
6	4	1	-1	1	72.69	68.89	5.24
10	5	2	0	0	70.35	69.88	0.67
4	6	1	1	-1	70.37	67.05	4.72
9	7	-2	0	0	33.44	37.44	11.95
13	8	0	0	-2	50.90	52.80	3.74
3	9	-1	1	-1	35.21	35.45	0.66
8	10	1	1	1	62.08	64.63	4.11
1	11	-1	-1	-1	67.09	60.95	9.15
7	12	-1	1	1	65.57	60.11	8.33
14	13	0	0	2	55.80	57.48	3.02
12	14	0	2	0	53.22	54.42	2.25
5	15	-1	-1	1	68.31	68.05	0.37
15	16	0	0	0	77.44	78.90	1.88
17	17	0	0	0	77.72	78.90	1.52
16	18	0	0	0	78.35	78.90	0.70

2. Materials and method

2.1. Bio-oil characterization

N. gaditana was chosen because of its high lipid content, which makes it a promising source for bio-oil production. This strain of microalgae has been reported to accumulate up to 68 % (%wt.) lipid content in the best cases [61]. The bio-oil used in this study (MBO) was provided by Neoalgae (Gijon, Spain).

The MBO's TAN was measured with a Metrohm 848 Tritino PLUS (accuracy ±0.01 mg KOH/g) following ASTM D664 to determine if esterification was necessary. The water content was also measured with a Metrohm 899 Karl Fischer coulometer (accuracy ±0.1 ppm).

The SL was determined using the method outlined by Callejón et al. [39]. The analysis provides the SL content per unit of lyophilized MBO and the lipid profile. This is achieved through a transesterification reaction with a solution of MeOH and acetyl chloride.

The lipid profile was analyzed using gas chromatography with flame ionization detector (GC-FID) following the UNE-EN 14103 standard after the transesterification reaction with acetyl chloride. The equipment used was a Clarus 690 (PerkinElmer) with an Elite-WAX column (30 m × 0.25 mm x 0.25 μm). The oven temperature was programmed in the following sequence: (1) hold at 60 °C for 2 min, (2) heat from 60 °C to 200 °C at 10 °C/min, (3) heat from 200 °C to 240 °C at 5 °C/min, (4) hold at 240 °C for 7 min. Hydrogen was used as the carrier gas, and the detector temperature was set at 250 °C with a flow rate of 2 mL/min. The injector was a split system with a set temperature of 250 °C and a sample volume of 1 μL. The sample was prepared at a concentration of 5 mg biodiesel per mL toluene. The detectable minimum concentration by GC-FID analysis was 1 %.

2.2. Transesterification reaction

2.2.1. Design of Experiments (DOE)

The MBO transesterification reaction was optimized using RSM. Design Expert 13 software was employed with a two-level factorial

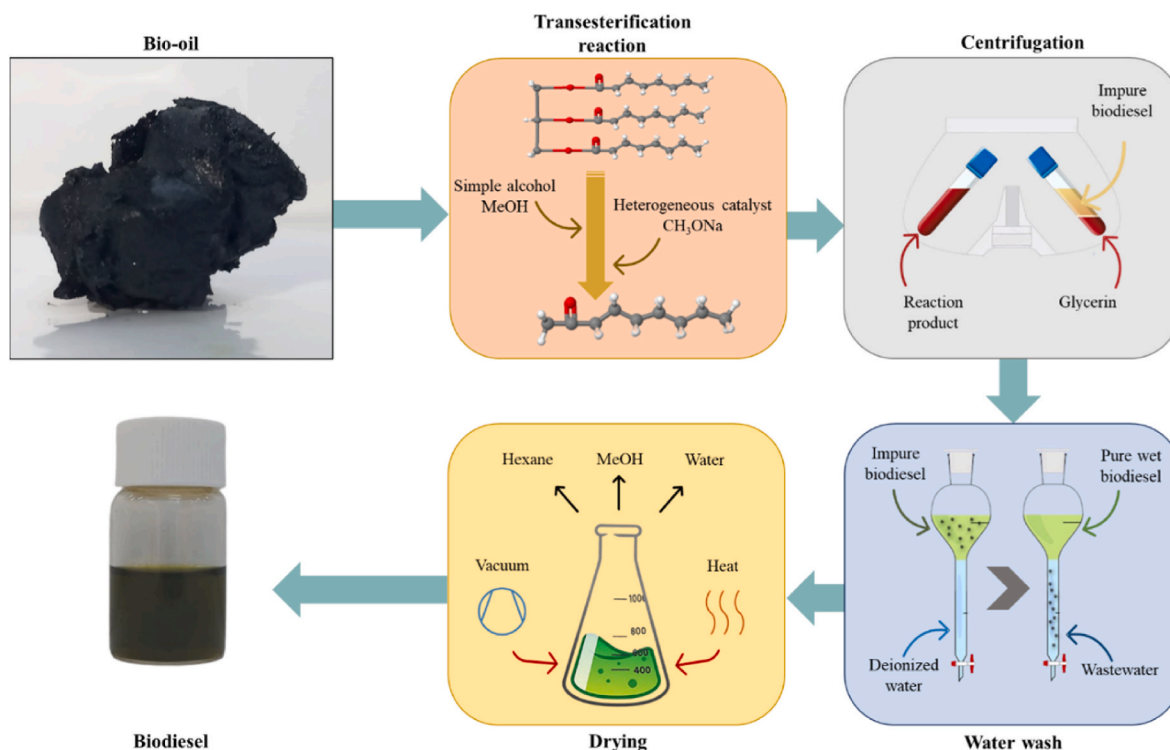


Fig. 3. Biodiesel purification process after transesterification.

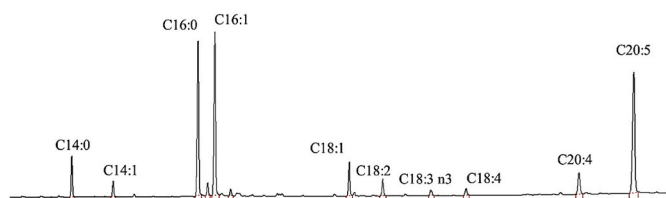


Fig. 4. Lipid profile chromatogram.

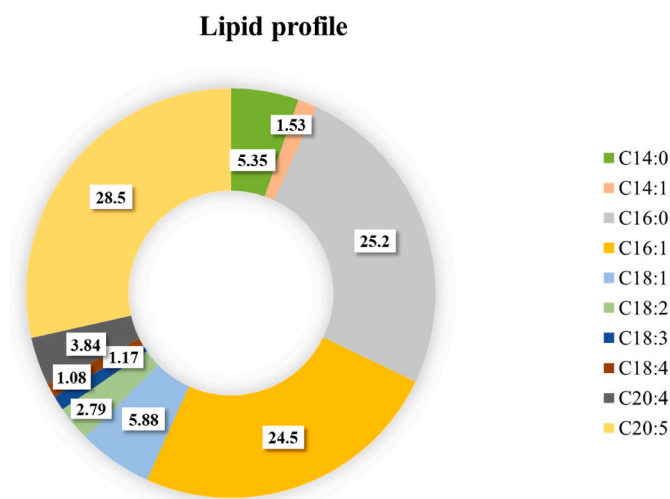
Fig. 5. Distribution of fatty acids in *N. gaditana*.

Table 4
Lipid content and fatty acids distribution of different of *N. gaditana* cultures.

SFA (%)	MUFA (%)	PUFA (%)	Total lipid content (%)	Ref.
30.55	31.91	35.6	35	Current
19	20.5	26.5	10.8	[67]
31.17	30.27	20.79	14	[20]
36.49	18.34	43.41	24.11	[66]
52.47	40.36	7.16	29.73	[68]
24.59	34.41	41	17.82	[69]
29.78	20.49	25.31	–	[70]

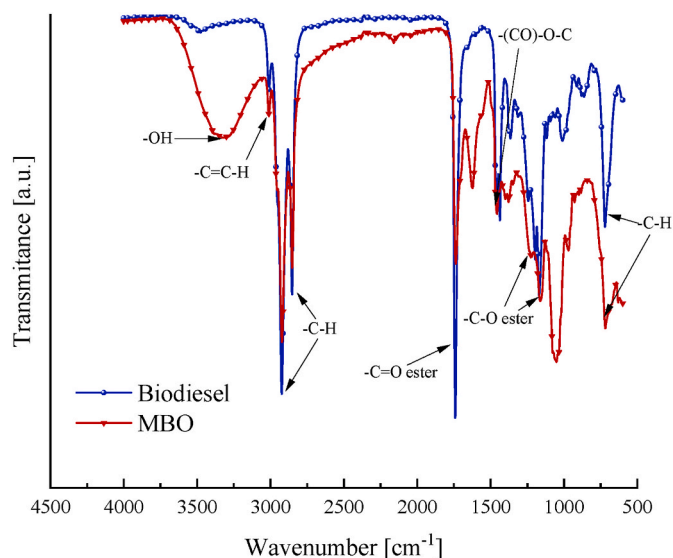


Fig. 6. FTIR spectra of bio-oil and biodiesel.

Table 5
ANOVA analysis of the fitting model for Y.

Source	df	F value	p value	Remark
<i>Model</i>	9	24.28	<0.0001	significant
A - Bio-oil:methanol ratio	1	61.52	<0.0001	
B - Reaction temperature	1	51.75	<0.0001	
C - Reaction time	1	1.29	0.2891	
AB	1	0.3973	0.5461	
AC	1	21.44	0.0017	
BC	1	9.02	0.0170	
A ²	1	50.70	<0.0001	
B ²	1	7.35	0.0266	
C ²	1	45.03	0.0002	
Residual	8			
Lack of Fit	5	105	0.0014	significant
<i>Model summary</i>	R ²	R ² (adj.)	R ² (pred.)	Adeq. Precision
	0.9647	0.9250	0.7366	17.3292

approach resulting in CCD [62]. Three numerical factors (input variables) were selected: bio-oil:methanol ratio (A), reaction temperature (B), and reaction time (C). Table 2 shows the values chosen for each input variable. They were chosen after a thorough evaluation of previous studies on biodiesel production from vegetable sources (Table 1). The parameter levels are coded as -1 (minimum), 0 (center), $+1$ (maximum), and $\pm \alpha$ (extreme star points), as shown in Table 2. The distance between α and the center point was set at 2. The study consisted of eighteen runs in total, including eight factorial design runs, six star points, and four replications of the center point, as detailed in Table 3 [63]. The FAME conversion (Y) was evaluated based on to Eq. (1). Optimization runs were conducted using 1 g of MBO as a simple size and 2 mL of hexane in the presence of the basic catalyst CH_3ONa at 1.5 %.

$$Y(\text{FAME conversion } \%) = \frac{\text{Amount transformed to FAME (g)}}{\text{Total SL amount convertible to FAME (g)}} \times 100 \quad \text{Eq.1}$$

2.2.2. Purification process

After completing the transesterification reaction is complete, a purification process is necessary to remove any impurities mixed with the biodiesel. The purification steps used in this study are illustrated in Fig. 3.

After the transesterification reaction, the resulting product was centrifuged at 7000 rpm for 10 min using a Microcen 24 - CE 202 to recover the biodiesel and remove the glycerol formed during the reaction. The liquid was then washed with deionized water until it reached a neutral pH. This step is essential to remove non-reacting MeOH, catalyst residues, and other impurities present in the MBO. Finally, the solution was transferred to a rotary evaporator (Hei-Vap Core, Heidolph) and evaporated at 60 °C and 20 mbar for 20 min to remove any remaining hexane, moisture, and MeOH.

2.3. Biodiesel physicochemical characterization

The GC-FID equipment was used to evaluate the FAME content for all runs. The quantitative analysis was performed according to UNE-EN 14103 using the procedure previously described for the lipid profile, with methyl nonadecanoate as an internal standard.

The density and dynamic viscosity of the samples were determined using a high-precision rotational viscometer (Stabinger SVM 3001) in accordance with the ASTM D7042 guidelines under atmospheric pressure conditions. The density was determined at a temperature of 20 °C, while the viscosity was determined at a temperature of 40 °C.

To determine the pour point (PP), Differential Scanning Calorimetry (DSC Mettler 822e 700) analysis was used, which has a heat flow accuracy of better than $\pm 2\%$ and a temperature accuracy of $\pm 1\text{ }^\circ\text{C}$. This

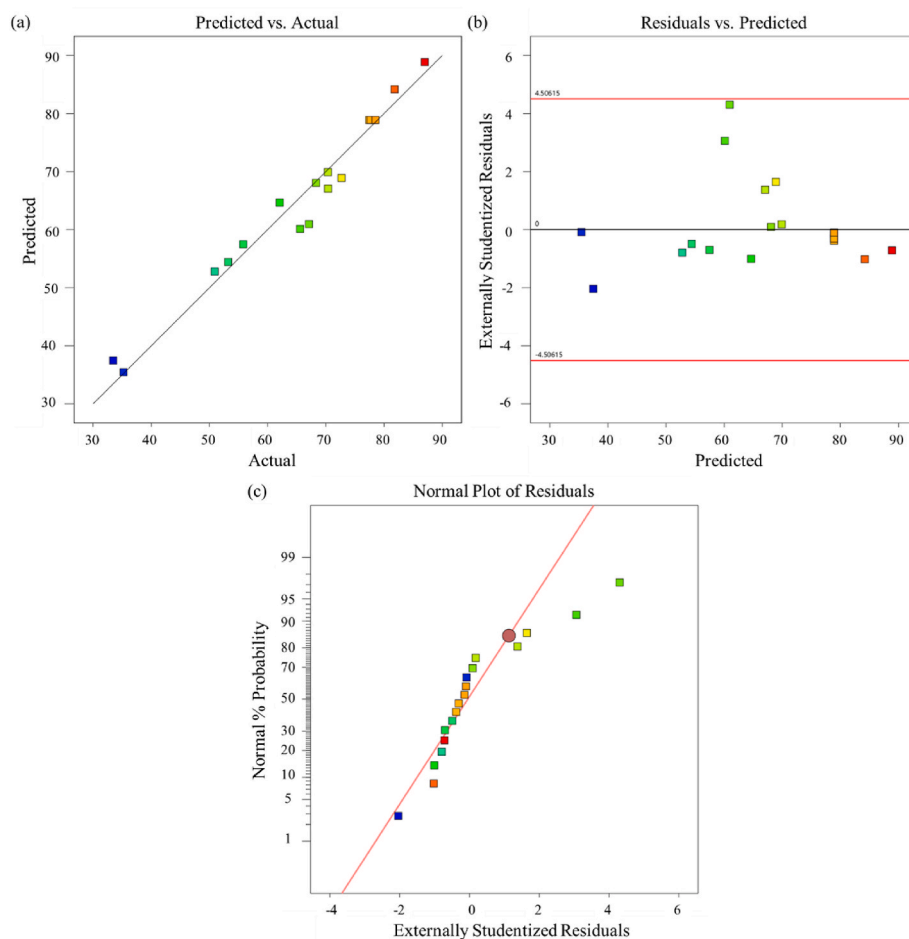


Fig. 7. Statistical analysis of the quadratic model generated for the response Y: (a) Predicted vs. Actuals; (b) Residuals vs. Predicted; (c) Normal plot of Residuals.

technique can provide a direct measurement of the change in enthalpy for a system during cooling, which can be approximated by the sample PP [64]. The procedure involves heating the sample to 50 °C at a steady rate of 10 °C/min and then holding it under isothermal conditions for 10 min. The system is then cooled to −50 °C at a steady rate of 10 °C/min under a nitrogen atmosphere. The PP value can be obtained at the maximum point of the curve by using Heat flow (W/g) versus temperature plots [65]. Additionally, the composition was analyzed using a Fourier Transform Infrared (FTIR) spectrometer (Varian 670-IR) with an accuracy of better than 0.07 cm^{-1} .

Thermal stability (TS) was evaluated using thermogravimetric analysis (TGA). The TA Instruments DSC SDT Q600 TGA & DSC was used for the analysis, which has a temperature accuracy of 0.001 °C (200–1300). The results were analyzed using TA Instruments Universal Analysis 2000 version software. The sample, approximately 6 mg, underwent dynamic scans at a constant heating rate of 20 °C/min from 25 to 600 °C under a nitrogen atmosphere at a flow rate of 50 mL/min. The sample's weight loss was plotted against time to obtain the onset temperature of decomposition.

The modified Cleveland Open Cup Tester, following EN ISO 2592 and ASTM D92 standards, was used to determine the flash point (FP). To determine the FP, 15 mL of biodiesel was gradually heated from room temperature in 5 °C increments until the FP was reached.

3. Results and discussion

3.1. Lipid profile and molecular structure

Fig. 4 displays the chromatogram of the lipid profile of the MBO,

while Fig. 5 shows the distribution of FAs. The FAs are evenly balanced between saturated (SFA), monounsaturated (MUFA), and polyunsaturated (PUFA). The GC-FID analysis of the biodiesel sample revealed three major peaks: C16:0 (25.2 %), C16:1 (24.5 %), and C20:5 (28.5 %). Additionally, minor peaks were found between C14:0 to C20:4, which accounted for 21.64 % of the sample. Microalgae oils often contain long-chain fatty acids and numerous double bonds, which are not typical of crop oils. However, a high concentration of double bonds in the molecular structure of fatty acids negatively impacts the material's oxidative stability. The presence of 70 % unsaturated FAs indicates poor resistance to oxidation.

The results are consistent with other cultures of the same species. Callejón et al. [39] and Tang et al. [66] reported a similar lipid profile, as shown in Fig. 4. However, the lipid content of the studied oil is higher than that reported in the literature (Table 4), reaching a lipid content of 35 %. This difference could be attributed to variations in culture and growth stage. Optimizing triglyceride production is essential for biodiesel conversion during these stages.

Fig. 6 shows the FTIR spectrum, highlighting the structural differences between the original bio-oil and the biodiesel. A band at 3342.03 cm^{-1} indicates the presence of alcohol compounds (-OH) used in the bio-oil extraction process. The increase of the characteristic bands at 2921.63 cm^{-1} and 2852.2 cm^{-1} is due to the increase in (-CH₃) alkanes, which result from the breaking of the triglyceride structure. The decrease in bands between 715 and 725 cm^{-1} is due to the loss of alkenes (-CH₂). The constant band at 3012.27 cm^{-1} is attributed to the (-C=C-) bonds. Additionally, esters (-C=O) at 1739.48 cm^{-1} , methyl acetate compounds ((CO)-O-C) at 1434.78 cm^{-1} , and other methyl compounds (-C-C(O)-C) at 1166.72 cm^{-1} are consistently present. The

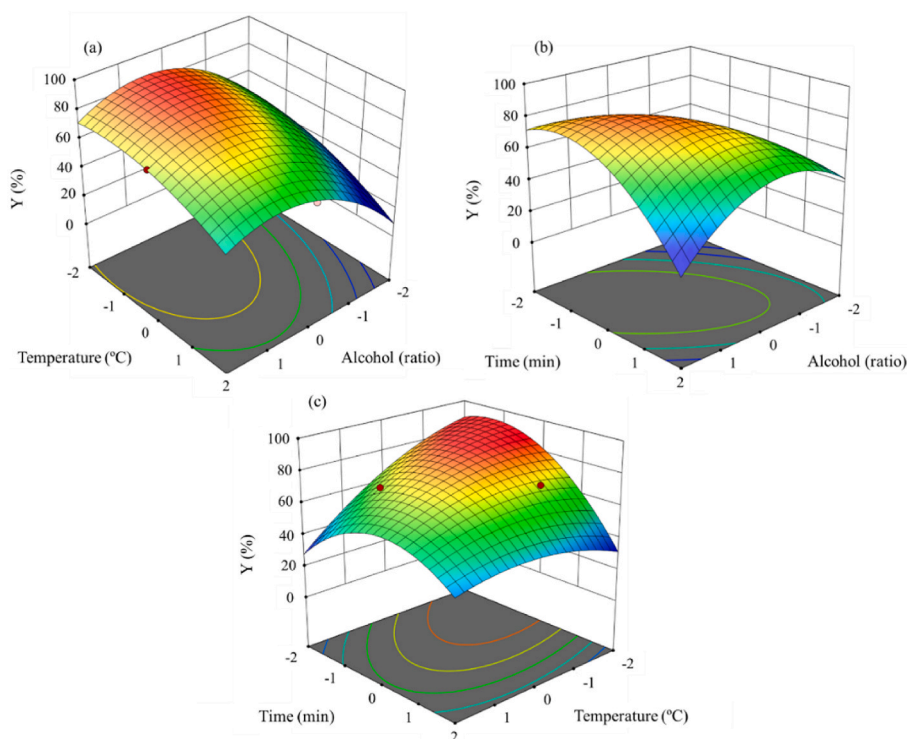


Fig. 8. Interaction between independent variables for response Y. (a) Interaction between temperature and alcohol ratio; (b) Interaction between reaction time and alcohol ratio; (c) Interaction between reaction time and temperature.

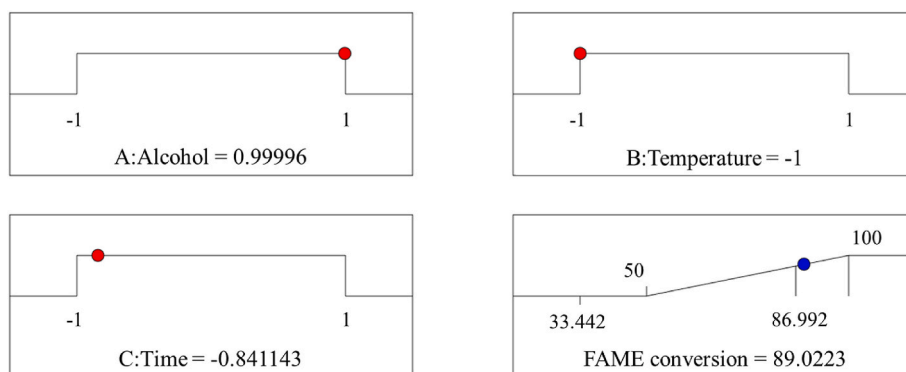


Fig. 9. Optimal conditions designed to produce desired results from independent variables using RSM-CCD.

spectrum of biodiesel obtained from *N. gaditana* agrees with those reported by other authors for the characterization of various vegetable biodiesels [34,51,57].

3.2. Optimization of transesterification reaction by RSM

3.2.1. Model adequacy check

After conducting the 18 tests, the empirical model correlating the input variables (coded) with Y (FAME conversion in %) was generated using a quadratic regression model fitted to Eq. (2):

$$Y = 78.90 + 8.11A - 7.44B + 1.17C + 0.9217AB - 6.77AC + 4.39BC - 6.31A^2 - 2.40B^2 - 5.94C^2 \tag{Eq.2}$$

The analysis of variance (ANOVA) was used to determine the interaction between each input variable and the response Y. The final results of the ANOVA analysis are summarized in Table 5.

The *F* and *p* values indicates the significance of the model [48]. An

F-value of 24.28 and a *p*-value less than 0.05 indicate that the model terms are significant. A value of R^2 of 0.9647 means that this quadratic regression model can explain over 96.47 % of the changes in the output response. The adjusted R^2 is also consistent with this value at 0.9250. Adequate precision (Adeq. Precision) measures the signal-to-noise ratio. A ratio greater than 4 is desirable. Therefore, a ratio of 17.3293 indicates sufficient signal to allow the model to be used to navigate the design space.

Fig. 7 shows the statistical analysis for the model. In particular, Fig. 7 (a) compares the values predicted by Eq. (2) with the experimental values. The predicted values closely match the actual data, indicating a reasonable correlation between them. The differences between the experimental and predicted values are less than 10 % for all the runs, except for one point (run 7). This result is consistent with the reported R^2 , R^2_{adj} and R^2_{pred} . The plot of the studentized residuals against the predicted values is shown in Fig. 7 (b). A random distribution of points is observed within the limit of ± 5 , indicating a constant discrepancy. This suggests that the models are suitable for their intended application

Table 6
Physicochemical characterization of bio-oil and biodiesel.

		Parameter					Ref.
		TAN mg KOH/g	Humidity ppm	PP °C	FP °C	TS (T _{onset}) °C	
Microalgae bio-oil (MBO)		1.11	1583.7	–	–	208.82	Current
Biodiesel	Microalgae	0.42	850	–7.2, –8.7	140–150	244.8	Current
	Soybean	0.34	–	–2	160	–	[72]
	Sunflower	0.41	–	–6	155	–	
	Corn	0.24	–	–5	140	–	
	Rice bran	0.71	–	–2	180	–	
	Olive	0.60	–	–6	155	–	
	Grape seed	–	–	–9	185	–	
	Edible waste	–	–	15	176	–	[73]
	Palm kernel	–	–	6	171	–	
	<i>Chlorella vulgaris</i>	–	–	–4.33	98.67	–	[74]
	Microalgae (not specified)	0.39	–	–10	165	–	[75]
	<i>Chlorella protothecoides</i>	0.224	183	–	183.9	–	[76]
<i>Spirulina platensis</i>	0.75	39	–9	189	330	[77]	

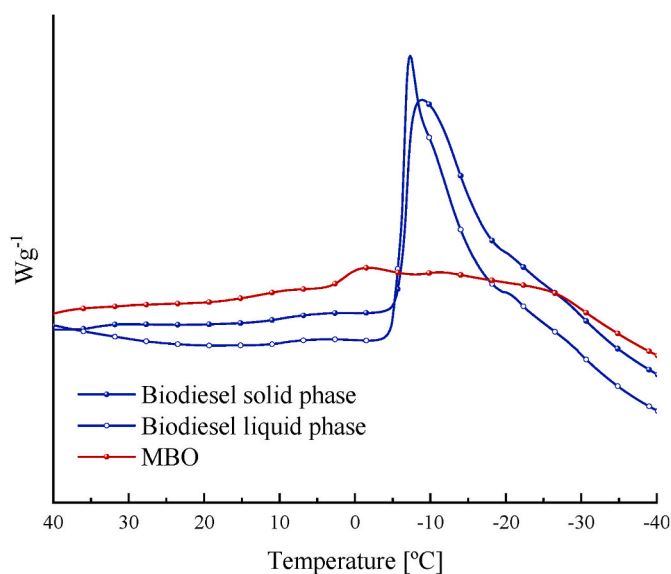


Fig. 10. DSC curve to study the PP of bio-oil and biodiesel.

without requiring modifications to reduce the scatter [71]. Finally, Fig. 7 (c) shows the normalized residuals of Y. The studentized residuals follow a linear distribution that predicts the accuracy of the quadratic model, generally with an S-shape generated by an additional transformation of the response [57]. The lack of precision between the actual and predicted values may be due to the low homogeneity of the sample, as the lipid content is only 35 % of the total of the sample. Additionally, the interference of foreign compounds from the microalgae oils such as liposoluble pigments (astaxanthin or zeaxanthin), may interfere and are difficult to remove during the biodiesel purification stage [67].

The study examines how the independent variables interact with the response using a 3D surface plot (see Fig. 8). The impact of the alcohol ratio is evident in Fig. 8 (a) and (b), where low alcohol ratios consistently lead to low reaction yields. However, an optimal point is reached in relation to the other parameters at a coded value of 1 (ratio 1:12). Fig. 8 (a) and (c) illustrate the relationship between temperature and other variables. Extreme temperatures, both high and low, can negatively affect reaction performance, as can reaction time. However, these variables tend to balance each other out, resulting in optimal performance between 50 and 70 °C and 67.5–105 min.

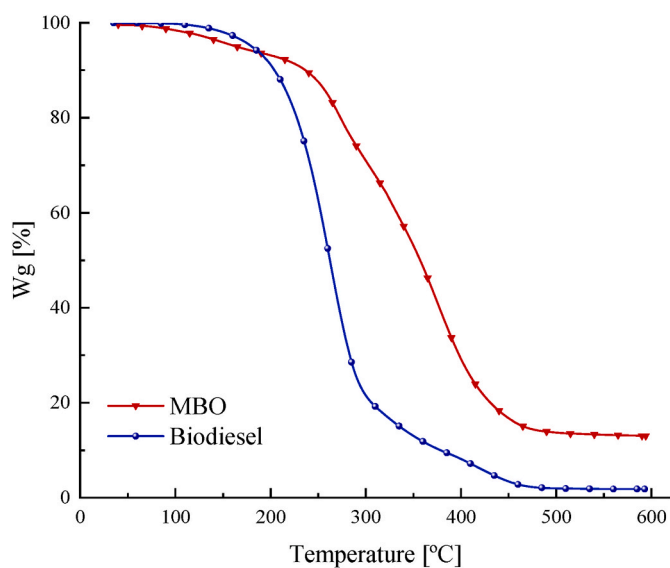


Fig. 11. TGA curve to study the thermal stability of bio-oil and biodiesel.

3.2.2. Optimized conditions of the RSM analysis

The ANOVA-validated model was used to determine the best conditions for producing biodiesel from the chosen microalgae, using Eq. (2). The input variables were limited to the bio-oil:MeOH ratio, reaction temperature, and reaction time within the study range (–1, 1), and the responses were maximized at 100 %. The software provided options with the highest FAME conversion, and the one that required the least amount of time and temperature was chosen. The model suggests that the experimental conditions shown in Fig. 9 are the best for achieving the highest reaction yield.

The transesterification reaction's optimal conditions were determined by decoding the independent variable set values. The reaction time was 75 min, and the temperature was 50 °C, with a bio-oil to alcohol ratio of 1:12. These test conditions resulted in an 87.2549 % FAME conversion, validating the generated model with a 2.20 % error between actual and predicted values.

3.3. Biodiesel physicochemical characterization

Table 6 presents the physicochemical properties of the current biodiesel, MBO, and vegetable and microalgae biodiesels from other

studies. Moreover, the fluid was found to have a density of 885 kg/m³ and a viscosity of 6.54 mPa s.

The low TAN values of the bio-oil simplified the preparation of the material before the transesterification reaction. A TAN of less than 2 mg KOH/g eliminated the need for a prior esterification due to the low levels of FFAs. The TAN slightly decreases after the reaction, possibly due to FFAs removal during purification or neutralization. Normal moisture levels for both compounds range from 850 to 1590 ppm, depending on ambient humidity. No drying was observed for the bio-oil.

The working temperature range of the biodiesel was determined through PP and FP measurements. Fig. 10 shows the behavior of both samples during the freezing point test. The bio-oil exhibited a broad exothermic band during the test, and no freezing temperature was defined. In contrast, the biodiesel separated into a liquid and a solid phase. Both phases showed a clear peak. The liquid phase was at −7.2 °C, and the solid phase was at −8.7 °C. These values are slightly lower than those reported for biodiesel from other vegetable sources (see Table 6).

During the biodiesel FP measurements, the sample ignited slightly at 130 °C but remained constant until the temperature range of 140–150 °C was reached. The ASTM D6751 standard [1] states that the FP in biodiesel is never lower than 120 °C, so the sample falls within the acceptable range. However, this value is significantly lower than those reported in Table 6 for biodiesel derived from vegetable sources.

The thermal stability analysis is presented in Fig. 11. The test results indicate that the biodiesel sample degraded completely at the maximum temperature used. The onset of temperature degradation for the biodiesel occurred at 244.8 °C, which was slightly better than the bio-oil that had a T_{onset} at 208.82 °C. Additionally, the biodiesel sample experienced rapid mass loss once it reached 200 °C, while the bio-oil counterpart maintained a constant and lower mass loss until it reached 250 °C. The bio-oil experiences a second phase of degradation at this point, with a steeper slope leading up to 450 °C. The initial loss of mass in the bio-oil may be attributed to the presence of organic solvents or impurities, as its water content was negligible.

Dantas et al. [78] obtained results that agree with ours. They studied the thermal stability variation of corn bio-oil after transesterification for biodiesel production. The degradation curve of the biodiesel showed the same trend as that of the bio-oil, with an onset of mass loss later. Corn oil degradation also proceeded in several phases, similar to our findings. Chand, P. et al. [79] evaluated the variation of the curve obtained from the thermal stability analysis of a soybean bio-oil/biodiesel blend. The trends of the two materials separately were similar to those reported in this study. The authors observed a decrease in thermal stability at higher concentrations of bio-oil. The results showed an improvement in thermal stability when biodiesel (FAME) was used instead of bio-oil (triglycerides).

Mostafa, S. et al. [77] reported higher FP and thermal stability values for a biodiesel derived from *S. platensis* microalgae compared to the biodiesel studied here (Table 6). This difference can be attributed to the FA distribution, as *S. platensis* has a higher percentage of PUFAs (2.11 %) which promote better tolerance to biofuel degradation, while the biodiesel studied here has a lower percentage of PUFAs (35.6 %).

4. Conclusions

The study investigated the use of microalgae *N. gaditana* as a biodiesel feedstock. Optimization of the transesterification reaction by RSM and physicochemical characterization of the biodiesel were carried out. The results showed that RSM is suitable for optimizing the synthesis of biodiesel from low homogeneity materials such as microalgae bio-oil. Using the optimal conditions from the model, the FAME conversion increased to 87.25 %, surpassing previous studies.

However, due to the high presence of double bonds in the fatty acid chains, the final biodiesel's oxidative stability is classified as low and

requires their removal. Additionally, the high degree of unsaturation resulted in a lower upper temperature limit, leading to a lower flash point and thermal stability. However, it improved the lower temperature limit by lowering the pour point when compared to first- and second-generation biodiesel.

Future research could explore the removal of double bonds in microalgae fatty acids through epoxidation or the use of antioxidant additives to mitigate their negative effects. Additionally, microalgae biodiesel could be investigated as a pour point depressant additive in diesel.

CRedit authorship contribution statement

C. Sanjurjo: Writing – original draft, Investigation, Conceptualization. **P. Oulego:** Supervision, Conceptualization. **M. Bartolomé:** Formal analysis, Data curation. **E. Rodríguez:** Writing – review & editing, Project administration, Investigation, Funding acquisition. **R. González:** Formal analysis, Data curation. **A. Hernández Battez:** Writing – review & editing, Project administration, Investigation, Funding acquisition, Conceptualization.

Data availability

Data will be made available on request.

Acknowledgements

This publication is part of the R&D project PID2022-136656NB-I00, funded by MICIU/AEI/10.13039/501100011033/and by “FEDER/UE”. The Foundation for the Promotion of Applied Scientific Research and Technology in Asturias (Spain) is also acknowledged for funding the contract of Claudia Sanjurjo at the University of Oviedo (Spain) [grant number: SV-PA-21-AYUD/2021/50987]. The authors of this work are grateful to the Institute of Industrial Technology of the University of Asturias (IUTA) for the financing of the project “OPTRANSESTERAL” (grant number SV-23-GIJON-1-05).

References

- [1] ASTM D6751- 7d, Standard Specification for Biodiesel Fuel Blend Stock (B100) for Middle Distillate Fuels, 2007.
- [2] G. Knothe, Biodiesel fuel quality and the ASTM standard, *Palmas* 31 (2010) 162–171.
- [3] M. Kanan, M.S. Habib, A. Shahbaz, A. Hussain, T. Habib, H. Raza, Z. Abusaf, R. Assaf, A grey-fuzzy programming approach towards socio-economic optimization of second-generation biodiesel supply chains, *Sustainability* 14 (2022) 10169.
- [4] D. Neupane, D. Bhattarai, Z. Ahmed, B. Das, S. Pandey, J.K.Q. Solomon, R. Qin, P. Adhikari, Growing jatropha (*Jatropha curcas* L.) as a potential second-generation biodiesel feedstock, *Inventions* 6 (2021) 60.
- [5] C. Sanjurjo, E. Rodríguez, J.L. Viesca, A.H. Battez, Influence of molecular structure on the physicochemical and tribological properties of biolubricants: a review, *Lubricants* 11 (2023) 380.
- [6] S. Brahma, B. Nath, B. Basumatary, B. Das, P. Saikia, K. Patir, S. Basumatary, Biodiesel production from mixed oils: a sustainable approach towards industrial biofuel production, *Chem. Eng. J. Adv.* 10 (2022) 100284.
- [7] N.S.M. Aron, K.S. Khoo, K.W. Chew, P.L. Show, W.H. Chen, T.H.P. Nguyen, Sustainability of the four generations of biofuels – a review, *Int. J. Energy Res.* 44 (2020) 9266–9282.
- [8] M.A.H. Shaah, M.S. Hossain, F.A.S. Allafi, A. Alsaedi, N. Ismail, M.O.A. Kadir, M. I. Ahmad, A review on non-edible oil as a potential feedstock for biodiesel: physicochemical properties and production technologies, *RSC Adv.* 11 (2021) 25018–25037.
- [9] W.C. Ulakpa, R.O.E. Ulakpa, M.C. Ekwunye, T.C. Egbosubi, Transesterification of non-edible oil and effects of process parameters on biodiesel yield, *Clean. Waste Syst.* 3 (2022) 100047.
- [10] K.S.H. Eldiehy, P. Bardhan, D. Borah, M. Gohain, M.A. Rather, D. Deka, M. Mandal, A comprehensive review on microalgal biomass production and processing for biodiesel production, *Fuel* 324 (2022) 124773.
- [11] N.K. Kondrasheva, A. Ereemeeva, Production of biodiesel fuel from vegetable raw materials, *J. Min. Inst.* 260 (2023) 248–256.
- [12] S. Vuttipongchaikij, Genetic manipulation of microalgae for improvement of biodiesel production, *Genom. Genet.* 5 (2012) 130–148.

- [13] M. Blanco-Vieites, D. Suárez-Montes, F. Delgado, M. Álvarez-Gil, A.H. Battez, E. Rodríguez, Removal of heavy metals and hydrocarbons by microalgae from wastewater in the steel industry, *Algal Res.* 64 (2022) 102700.
- [14] M. Blanco-Vieites, D. Suárez-Montes, A. Hernández Battez, E. Rodríguez, Enhancement of *Arthrospira* sp. culturing for sulfate removal and mining wastewater bioremediation, *Int. J. Phytoremediation* 25 (9) (2023) 1116–1126. <https://doi.org/10.1080/15226514.2022.2135680>.
- [15] M.S.J. Ollia, M. Azin, A.A. Sepahi, N. Moazzami, Miniaturized culture method for the statistical study of growth rate and carbohydrate content of *Picochlorum* sp. D8 isolated from the Persian Gulf, *Renew. Energy* 149 (2020) 479–488.
- [16] L. Peng, D. Fu, H. Chu, Z. Wang, H. Qi, Biofuel production from microalgae: a review, *Environ. Chem. Lett.* 18 (2020) 285–297.
- [17] European Federation for Transport and Environment, The Basis for Biofuel Policy Post-2020, 2020.
- [18] IEA50, Total Biofuel Production by Feedstock, Main Case, 2021–2027, 2022.
- [19] P.G. Roessler, L.M. Brown, T.G. Dunahay, D.A. Heacox, E.E. Jarvis, J.C. Schneider, S.G. Talbot, K.G. Zeiler, Genetic Engineering Approaches for Enhanced Production of Biodiesel Fuel from Microalgae, vol. 14, National Renewable Energy Laboratory, 1994, pp. 255–270.
- [20] L.I. Farfan-Cabrera, M. Franco-Morgado, A. González-Sánchez, J. Pérez-González, B.M. Marín-Santibáñez, Microalgae biomass as a new potential source of sustainable green lubricants, *Molecules* 27 (2022) 1205.
- [21] T.M.M. Bernaerts, L. Gheysen, I. Foubert, M.E. Hendrickx, A.M. Van Loey, Evaluating microalgal cell disruption upon ultra high pressure homogenization, *Algal Res.* 42 (2019) 101616.
- [22] A. Hernández-Pérez, J.I. Labbé, Microalgae, culture and benefits, *Rev. Biol. Mar. Oceanogr.* 49 (2014) 157–173.
- [23] M.K. Enamala, S. Enamala, M. Chavali, J. Donepudi, R. Yadavalli, B. Kolapalli, T. V. Aradhya, J. Velpuri, C. Kuppam, Production of biofuels from microalgae - a review on cultivation, harvesting, lipid extraction, and numerous applications of microalgae, *Renew. Sustain. Energy Rev.* 94 (2018) 49–68.
- [24] C. Onumaegbu, A. Alaswad, C. Rodriguez, A.G. Olabi, Optimization of pre-treatment process parameters to generate biodiesel from microalga, *Energies* 11 (2018) 806.
- [25] S. Zhang, L. Zhang, G. Xu, F. Li, X. Li, A review on biodiesel production from microalgae: influencing parameters and recent advanced technologies, *Front. Microbiol.* 13 (2022) 970028.
- [26] P.L. Show, M.S.Y. Tang, D. Nagarajan, T.C. Ling, C.W. Ooi, J.S. Chang, A holistic approach to managing microalgae for biofuel applications, *Int. J. Mol. Sci.* 18 (2017) 215.
- [27] W. Wang, H. Liu, F. Li, H. Wang, X. Ma, J. Li, L. Zhou, Q. Xiao, Effects of unsaturated fatty acid methyl esters on the oxidation stability of biodiesel determined by gas chromatography-mass spectrometry and information entropy methods, *Renew. Energy* 175 (2021) 880–886.
- [28] G.R. Stansell, V.M. Gray, S.D. Sym, Microalgal fatty acid composition: implications for biodiesel quality, *J. Appl. Phycol.* 24 (2012) 791–801.
- [29] N.N. Zulu, K. Zienkiewicz, K. Vollheyde, I. Feussner, Current trends to comprehend lipid metabolism in diatoms, *Prog. Lipid Res.* 70 (2018) 1–16.
- [30] E.G. Giakoumis, A statistical investigation of biodiesel physical and chemical properties, and their correlation with the degree of unsaturation, *Renew. Energy* 50 (2013) 858–878.
- [31] M. Salaheldien, A.A. Mariod, M.K. Aroua, S.M.A. Rahman, M.E.M. Soudagar, I.M. R. Fattah, Current state and perspectives on transesterification of triglycerides for biodiesel production, *Catalysts* 11 (2021) 1121.
- [32] G.F. Silva, F.L. Camargo, A.L.O. Ferreira, Application of response surface methodology for optimization of biodiesel production by transesterification of soybean oil with ethanol, *Fuel Process. Technol.* 92 (2011) 407–413.
- [33] J.W.Y. Lee, W.Y. Chia, W.J. Ong, W.Y. Cheah, S.S. Lim, K.W. Chew, Advances in catalytic transesterification routes for biodiesel production using microalgae, *Sustain. Energy Technol. Assessments* 52 (2022) 102336.
- [34] C.S. Latchugata, R.V. Kondapaneni, K.K. Patluri, U. Virendra, S. Vedantam, Kinetics and optimization studies using Response Surface Methodology in biodiesel production using heterogeneous catalyst, *Chem. Eng. Res. Des.* 135 (2018) 129–139.
- [35] V. Singh, L. Belova, B. Singh, Y.C. Sharma, Biodiesel production using a novel heterogeneous catalyst, magnesium zirconate (Mg₂Zr₅O₁₂): process optimization through response surface methodology (RSM), *Energy Convers. Manag.* 174 (2018) 198–207.
- [36] D.N. Thoai, C. Tongurai, K. Prasertsit, A. Kumar, A novel two-step transesterification process catalyzed by homogeneous base catalyst in the first step and heterogeneous acid catalyst in the second step, *Fuel Process. Technol.* 168 (2017) 97–104, <https://doi.org/10.1016/j.fuproc.2017.08.014>.
- [37] A.K. Azad, S.C. Sharma, M.G. Rasul, Clean Energy for Sustainable Development: Comparisons and Contrasts of New Approaches, 2017.
- [38] X. Li, H. Xu, Q. Wu, Large-scale biodiesel production from microalga *Chlorella protothecoides* through heterotrophic cultivation in bioreactors, *Biotechnol. Bioeng.* 98 (2007) 764–771.
- [39] M.J.J. Callejón, A.R. Medina, M.D.M. Sánchez, E.H. Peña, L.E. Cerdán, P.A. G. Moreno, E.M. Grima, Extraction of saponifiable lipids from wet microalgal biomass for biodiesel production, *Bioresour. Technol.* 169 (2014) 198–205.
- [40] C. Sronsri, W. Sittipol, K. U-yen, Optimization of biodiesel production using magnesium pyrophosphate, *Chem. Eng. Sci.* 226 (2020) 115884, <https://doi.org/10.1016/j.ces.2020.115884>.
- [41] A. Prabu, I. Premkumar, A. Pradeep, Production of ricebran biodiesel by the bubble wash method, *Int. J. Ambient Energy* 42 (2021) 981–984.
- [42] N. Hasanudin, N.A. Ghani, A.H.A. Rahim, N.S. Azman, N.A. Rosdi, A.N. Masri, Optimization and kinetic studies on biodiesel conversion from *Chlorella vulgaris* microalgae using pyrrolidinium-based ionic liquids as a catalyst, *Catalysts* 12 (2022) 277.
- [43] S.T. Al-Humairi, J.G.M. Lee, M. Salihu, A.P. Harvey, Biodiesel production through acid catalyst in situ reactive extraction of *Chlorella vulgaris* foamate, *Energies* 15 (2022) 4482.
- [44] O. Paladino, M. Neviani, Sustainable biodiesel production by transesterification of waste cooking oil and recycling of wastewater rich in glycerol as a feed to microalgae, *Sustainability* 14 (2022) 273.
- [45] X. Miao, Q. Wu, Biodiesel production from heterotrophic microalgal oil, *Bioresour. Technol.* 97 (2006) 841–846.
- [46] T.A. Saavedra, L.B. Bueno-Borges, N. Sangaletti-Gerhard, S.M. de Alencar, M.A. B. Regitano-d'Arce, Optimized conventional and ultrasound-assisted ethyl transesterification of *Jatropha* (*Jatropha curcas*) and palm (*Elaeis guineensis*) oil mixtures, *Chem. Eng. Commun.* 209 (2022) 1482–1495.
- [47] J. Calero, D. Luna, C. Luna, F.M. Bautista, A.A. Romero, A. Posadillo, R. Estevez, Optimization by response surface methodology of the reaction conditions in 1,3-selective transesterification of sunflower oil, by using CaO as heterogeneous catalyst, *Mol. Catal.* 484 (2020).
- [48] S. Zou, H. Zhang, J. Wang, Ultrasound-assisted pickering interfacial catalysis for transesterification: optimization of biodiesel yield by response surface methodology, *J. Oleo Sci.* 72 (2023) 233–243.
- [49] K. Khiri, L. Tarabet, S. Awad, K. Loubar, R. Mahmoud, M. Tazerout, Optimization of *Pistacia lentiscus* oil transesterification process using central composite design, *Waste Biomass Valorization* 10 (2019) 2575–2581.
- [50] M. Mohamad, N. Ngadi, S.L. Wong, M. Jusoh, N.Y. Yahya, Prediction of biodiesel yield during transesterification process using response surface methodology, *Fuel* 190 (2017) 104–112.
- [51] F.A. Aisien, E.T. Aisien, Modeling and optimization of transesterification of rubber seed oil using sulfonated CaO derived from giant African land snail (*Achatina fulica*) catalyst by response surface methodology, *Renew. Energy* 207 (2023) 137–146.
- [52] D. Beyene, M. Abdulkadir, A. Befekadu, Production of biodiesel from mixed Castor seed and microalgae oils: optimization of the production and fuel quality assessment, *Int. J. Chem. Eng.* 2022 (2022) 1–14.
- [53] Y. Nan, J. Liu, R. Lin, L.L. Tavarides, Production of biodiesel from microalgae oil (*Chlorella protothecoides*) by non-catalytic transesterification in supercritical methanol and ethanol: process optimization, *J. Supercrit. Fluids* 97 (2015) 174–182.
- [54] N. Nirmala, S.S. Dawn, Optimization of *Chlorella variabilis* MK039712.1 lipid transesterification using Response Surface Methodology and analytical characterization of biodiesel, *Renew. Energy* 179 (2021) 1663–1673.
- [55] H. Mohamadzadeh Shirazi, J. Karimi-Sabet, C. Ghotbi, Biodiesel production from *Spirulina* microalgae feedstock using direct transesterification near supercritical methanol condition, *Bioresour. Technol.* 239 (2017) 378–386.
- [56] H. Ramírez, H. Arteaga, R. Siche, Optimización del proceso de obtención de biodiesel a partir de colza silvestre (*Brassica Campestris*) Process optimization of biodiesel production from wild rapeseed (*Brassica campestris*), *Sci. Agropecu.* 3 (2012) 35–44.
- [57] S. Sohail, M.W. Mumtaz, H. Mukhtar, T. Touqeer, M.K. Anjum, U. Rashid, W.A.W. A.K. Ghani, T.S.Y. Choong, Spirogyra oil-based biodiesel: response surface optimization of chemical and enzymatic transesterification and exhaust emission behavior, *Catalysts* 10 (2020) 1–12.
- [58] T. Sangsawang, N. Rongrat, A. Yothayuth, Optimization for biodiesel production by transesterification with electric fields, *Eng. J.* 25 (2021) 261–268.
- [59] M.D. Macías-Sánchez, A. Robles-Medina, M.J. Jiménez-Callejón, E. Hita-Peña, L. Estéban-Cerdán, P.A. González-Moreno, E. Navarro-López, E. Molina-Grima, Optimization of biodiesel production from wet microalgal biomass by direct transesterification using the surface response methodology, *Renew. Energy* 129 (2018) 141–149.
- [60] M.D. Macías-Sánchez, A. Robles-Medina, E. Hita-Peña, M.J. Jiménez-Callejón, L. Estéban-Cerdán, P.A. González-Moreno, E. Molina-Grima, Biodiesel production from wet microalgal biomass by direct transesterification, *Fuel* 150 (2015) 14–20.
- [61] V.C. Akubode, K.N. Nwaigwe, E. Dintwa, Production of biodiesel from microalgae via nanocatalyzed transesterification process: a review, *Mater. Sci. Energy Technol.* 2 (2019) 216–225.
- [62] M.J. Anderson, P.J. Whitcomb, Optimizing Processes Using Response Surface Methods for Design of Experiments Second Edition RSM Simplified, 2016.
- [63] N.H. Zabaruddin, L.C. Abdullah, N.H. Mohamed, T.S.Y. Choong, Optimization using response surface methodology (RSM) for biodiesel synthesis catalyzed by radiation-induced kenaf catalyst in packed-bed reactor, *Processes* 8 (2020) 1–18.
- [64] A. Adhvariyu, S.Z. Erhan, J.M. Perez, Wax appearance temperatures of vegetable oils determined by differential scanning Calorimetry: effect of triacylglycerol structure and its modification, *Thermochim. Acta* 395 (2002) 191–200.
- [65] N.H. Jayadas, K.P. Nair, Coconut oil as base oil for industrial lubricants-evaluation and modification of thermal, oxidative and low temperature properties, *Tribol. Int.* 39 (2006) 873–878.
- [66] Y. Tang, J.N. Rosenberg, M.J. Betenbaugh, F. Wang, Optimization of one-step in situ transesterification method for accurate quantification of epa in *Nannochloropsis gaditana*, *Appl. Sci.* 6 (2016).
- [67] E.H. Peña, A.R. Medina, M.J.J. Callejón, M.D.M. Sánchez, L.E. Cerdán, P.A. G. Moreno, E.M. Grima, Extraction of free fatty acids from wet *Nannochloropsis gaditana* biomass for biodiesel production, *Renew. Energy* 75 (2015) 366–373.

- [68] Q. Hu, W. Xiang, S. Dai, T. Li, F. Yang, Q. Jia, G. Wang, H. Wu, The influence of cultivation period on growth and biodiesel properties of microalga *Nannochloropsis gaditana* 1049, *Bioresour. Technol.* 192 (2015) 157–164.
- [69] N. Nogueira, F.J.A. Nascimento, C. Cunha, N. Cordeiro, *Nannochloropsis gaditana* grown outdoors in annular photobioreactors: operation strategies, *Algal Res.* 48 (2020) 101913.
- [70] S. Torres, G. Acien, F. García-Cuadra, R. Navia, Direct transesterification of microalgae biomass and biodiesel refining with vacuum distillation, *Algal Res.* 28 (2017) 30–38.
- [71] Y. Zhang, S. Niu, C. Lu, Z. Gong, X. Hu, Catalytic performance of NaAlO₂/γ-Al₂O₃ as heterogeneous nanocatalyst for biodiesel production: optimization using response surface methodology, *Energy Convers. Manag.* 203 (2020) 112263.
- [72] B. Bazooyar, A. Ghorbani, A. Shariati, Physical properties of methyl esters made from alkali-based transesterification and conventional diesel fuel, *Energy Sources, Part A Recovery, Util. Environ. Eff.* 37 (2015) 468–476.
- [73] R. Foroutan, H. Esmaeili, S.M. Mousavi, S.A. Hashemi, G. Yeganeh, The physical properties of biodiesel-diesel fuel produced via transesterification process from different oil sources, *Phys. Chem. Res.* 7 (2019) 415–424.
- [74] K.O. Nwanya, P.A.C. Okoye, V.I.E. Ajiwe, Biodiesel potentials of *Chlorella vulgaris* oil, *Niger. Res. J. Chem. Sci.* 9 (2021).
- [75] O.S. Onyinyechi, D.T. Obinna, Comparative Assessment of Biodiesel Produced from Microalgae, Used Vegetable Oil and Fossils, vol. 8, 2020, pp. 1–10.
- [76] F.R.M. Batista, K.W. Lucchesi, N.D.D. Carareto, M.C.D. Costa, A.J.A. Meirelles, Properties of microalgae oil from the species *Chlorella protothecoides* and its ethylic biodiesel, *Braz. J. Chem. Eng.* 35 (2018) 1383–1394.
- [77] S.S.M. Mostafa, N.S. El-Gendy, Evaluation of fuel properties for microalgae *Spirulina platensis* biodiesel and its blends with Egyptian petro-diesel, *Arab. J. Chem.* 10 (2017) S2040–S2050.
- [78] M.B. Dantas, M.M. Conceição, Fernandes Jr., Thermal and kinetic study of corn biodiesel obtained by the methanol and ethanol routes, *J. Therm. Anal. Calorim.* 87 (2007) 835–839.
- [79] P. Chand, C.V. Reddy, J.G. Venkat, T. Wang, D. Grewell, Thermogravimetric quantification of biodiesel produced via alkali catalyzed transesterification of soybean oil, *Energy Fuel.* 23 (2009) 989–992.